J Electr Eng Technol Vol. 7, No. 6: 834-844, 2012
http://dx.doi.org/10.5370/JEET.2012.7.6.834

ISSN(Print) 1975-0102
ISSN(Online) 2093-7423

Intelligent Coordination Method of Multiple Distributed Resources for Harmonic Current Compensation in a Microgrid

Hyun-Koo Kang*, Choel-Hee Yoo, Il-Yop Chung†, Dong-Jun Won*** and Seung-Il Moon***

Abstract – Nonlinear electronic loads draw harmonic currents from the power grids that can cause energy loss, miss-operation of power equipment, and other serious problems in the power grids. This paper proposes a harmonic compensation method using multiple distributed resources (DRs) such as small distributed generators (DGs) and battery energy storage systems (BESSs) that are integrated to the power grids through power inverters. For harmonic compensation, DRs should inject additional apparent power to the grids so that certain DRs, especially operated in proximity to their rated power, may possibly reach their maximum current limits. Therefore, intelligent coordination methods of multiple DRs are required for efficient harmonic current compensation considering the power margins of DRs, energy cost, and the battery state-of-charge. The proposed method is based on fuzzy multi-objective optimization so that DRs can cooperate with other DRs to eliminate harmonic currents with optimizing mutually conflicting multi-objectives.

Keywords: Harmonic compensation, Multiple distributed resources control, Multi-objective optimization, Microgrid

1. Introduction

Power system harmonics are often caused by nonlinear loads that draw significant non-sinusoidal currents from the power grids. Rectifiers, switch-mode power supplies, motor drives, and arc furnaces are notorious for harmonic producing loads. Harmonics might lead to detrimental effects in power grids such as heating in transformer and machines, mal-operation of controllers and protection relays, and interference with radio-frequency circuits especially when harmonic frequencies induce resonant problems in power grids [1-3]. Therefore, there have been many efforts to regulate harmonic current emitted to the grids [4-5].

Power inverters can effectively compensate harmonics because they can flexibly shape the output voltages and currents into certain desired waveforms by fast switching of the power-electronic devices [6-8]. Shunt active power filters are one of the effective power inverter-based harmonic compensators.

Recently, due to energy reliability and sustainability issues, DRs such as small distributed generators (DGs), renewable energy sources (RESs) and battery energy storage systems (BESSs) are integrated to the grids [9-11]. Most DRs are interconnected to the grids through power inverters that are required for synchronization and power control. This paper proposes an effective harmonic compensation method by utilizing the multiple power inverter-based DRs in place of power filters. One of the possible advantages of the proposed method is that the installation cost of additional power filters can be relieved. In addition, we have multiple harmonic compensators instead of one solely devoted harmonic filter in the microgrid.

There are two important issues of the harmonic compensation using the power inverter-based DRs. First, when the power inverters compensate the harmonics in the grids, the injection current of the power inverters should be increased [8]. Therefore, the power margin of each power inverters should be measured accurately and the amount of harmonic compensation should be distributed appropriately to multiple DRs. Second, DRs have diverse control scheme depending on their types and operational strategies [12-13]. Therefore, the multiple objective functions should be considered to coordinate of multiple DRs.

This paper introduces a new intelligent coordination method based on fuzzy multi-objective optimization method. Fuzzy-based optimization methods have been applied to power system coordination problems such as reactive power control, power scheduling, network restoration, and other power system issues [14-16]. To solve our coordination problem, this paper formulates the multi-objective optimization problem using fuzzy sets like as in the previous studies. In addition, the fuzzy

† Corresponding Author: School of Electrical Engineering, Kookmin University, Korea. (chung@kookmin.ac.kr)
* School of Electrical Engineering, Seoul National University, Korea. (khyun9@powerlab.snu.ac.kr, moonsi@plaza.snu.ac.kr)
** School of Electrical Engineering, Kookmin University, Korea. (cheol21c@kookmin.ac.kr)
*** Dept. of Electrical Engineering, INHA University, Korea. (djwon@inha.ac.kr)
Received: December 8, 2011; Accepted: September 10, 2012

membership functions are designed corresponding to the design criteria. The proposed method can maximize the overall satisfaction degree of harmonic compensation of DRs. The performance of the proposed coordination method is verified via simulation studies with a detailed simulation model of a microgrid including a PV, two small DGs, a BESS and a nonlinear load.

2. Microgrid Configuration

2.1 Microgrid configuration and operation

Microgrids are state-of-the-art power distribution networks that consist of multiple DRs and sensitive power loads. The goal of microgrid operation is to provide electric power to the loads with high reliability regardless of abnormal operations in the power grids. From the perspective of the grids, microgrids can be considered as autonomous cells that can be operated by independent operators based on power exchange contracts. This configuration gives advantages to both the power grids and the microgrids [9-11]. Fig. 1 illustrates a single-line diagram of a microgrid that contains a photovoltaic (PV) system, two small inverter-interfaced DGs, a BESS and a nonlinear load.

The nonlinear load represents electronic loads that commonly employ power conversion circuits such as rectifiers and switching-mode power supplies. They draw significant harmonic currents steadily during their operation. The power grid and the neighbor power facility can suffer severe harmonic problems. A common countermeasure is to install passive or active power filters near the nonlinear loads to keep harmonic currents from flowing into the grid and the adjacent feeders. Passive filters can be the cheapest solution when it comes to single harmonic component elimination but it is hard to compensate various harmonic components at the same time. Active power filters are an effective solution but the installation and management are costly. The basic idea of this paper is to utilize the local inverter-interfaced DRs to compensate multiple harmonic components. The system

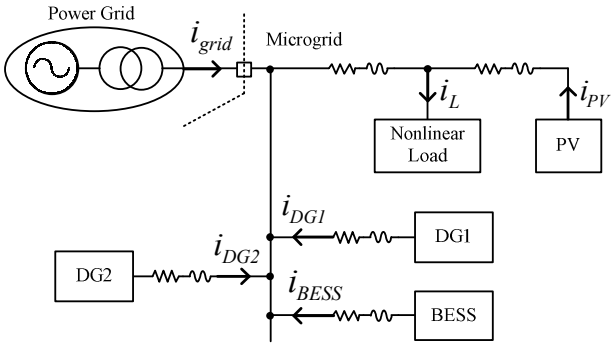

Fig. 1. Microgrid single-line diagram showing grid, load, and DR current flow

operator can save the installation cost of additional power filters and also can have multiple distributed compensators in the microgrid.

2.2 PV system model

The PV module can be modeled as a diode circuit as shown in Fig. 2 [17]. The PV system generates dc power determined mainly by the level of solar radiation. The output power is then converted to ac power for injection into the grid through a dc-dc boost converter and a dc-ac power inverter as shown in Fig. 3. A boost converter with 5 kHz PWM switching is used for the DC-DC converter and a three-level three-phase inverter with 10 kHz switching is used as the grid converter. To fully utilize the PV system, maximum power-point tracking (MPPT) algorithms are normally used in the controller of the boost converter. Among various MPPT algorithms, the perturbation and observation (P&O) algorithm for the dc-dc converter are used in this paper [18-20].

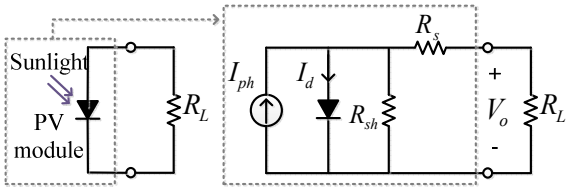

Fig. 2. Equivalent circuit model of a PV module

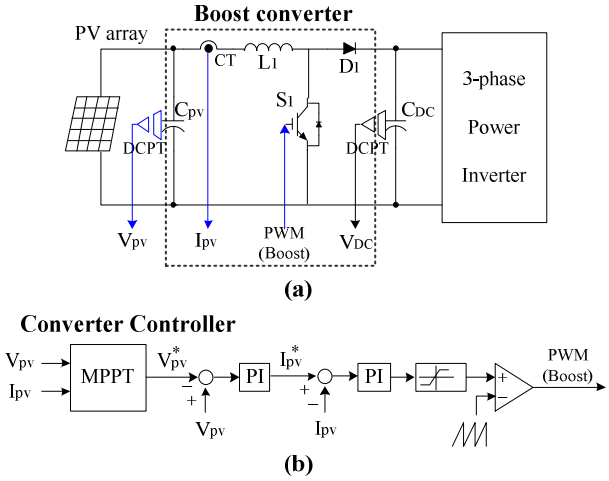

Fig. 3. Power conversion circuit and converter controller with MPPT algorithm

2.3 Battery energy storage system (BESS) model

Recent progress in battery technology enables large size BESSs to be integrated to the power grids. BESSs can compensate for the instant power mismatch in a microgrid and the intermittent power output of renewable energy resources and also ancillary services [21]. Fig. 4 illustrates the equivalent model the BESS that contains a Li-ion

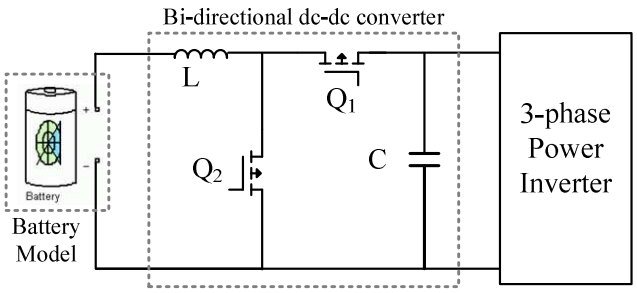

Fig. 4. Battery equivalent model and bi-directional dc-dc converter for battery charging and discharging

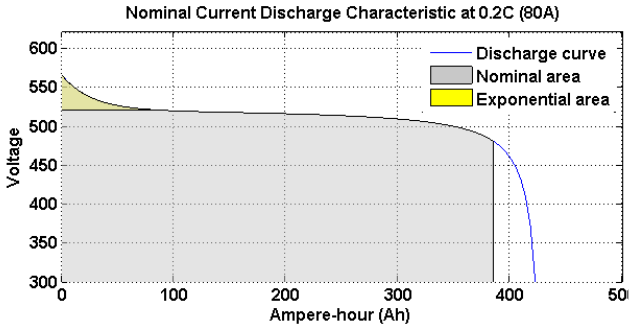

Fig. 5. Battery discharging characteristics of Li-ion battery cell

battery model, a bi-directional dc-dc converter, and a three-phase power inverter. This paper used the battery model provided by MATLAB/Simulink. The nominal voltage of the battery model is 480V and the rated capacity is 400 Ah, which means the battery size is 200kWh. Fig. 5 shows the characteristic curves for battery discharging characteristics of a lithium-ion battery cell used in this paper under the condition of 560V as the fully charged voltage and 80 A (about 40kW rating) as nominal discharging current.

The control scheme for the charging and discharging dc-dc converter for the battery model is as follows. During the charging period, the switch Q_1 operates as a switching device whereas the Q_2 acts as a diode of a buck converter. Therefore, the dc-dc converter operates in the buck mode. As shown in Fig. 5, the dc-dc converter controls the charging current in the beginning. When the battery voltage reaches a certain level, the dc-dc converter controls the battery voltage as constant. During the discharging period, the dc-dc converter operates in the boost mode: the Q_2 switches while the Q_1 operates as a diode of a boost converter. In the discharging characteristics, there is an inflection point in the battery discharging characteristics. In normal operation, the battery should not be discharged beyond the inflection point as seen in Fig. 5.

The state of charge (SOC) of a battery is an index for the available capacity of the battery compared to its rated capacity. The SOC of the battery should be maintained between 30% and 100% for longer battery life [18].

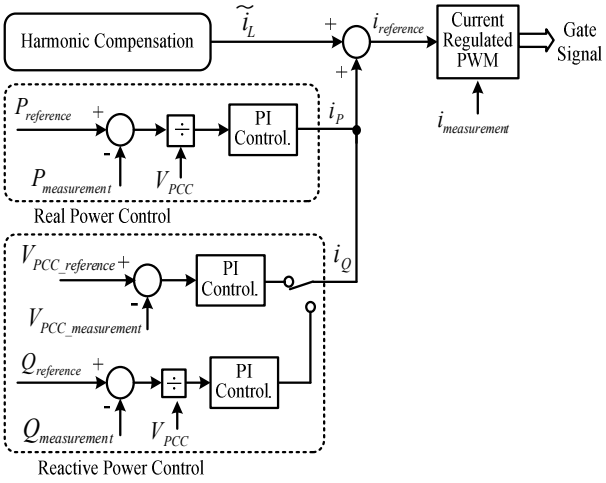

Fig. 6. Control block diagram of three-phase power inverter for injection current control

2.4 Three-phase power inverter model

To compensate harmonic current, the three-phase power inverters can utilize the current-regulated pulse width modulation (CRPWM) scheme. Fig. 6 illustrates the control block diagram of the power inverters using the CRPWM scheme. The reference current of the power inverter can be determined by summing the real and reactive power generation currents and the harmonic compensation current. In order to calculate the reference signal of the harmonic compensation currents, the harmonic components should be evaluated. The detailed harmonic identification algorithm used in this paper will be explained in Section 3.2.

3. Harmonic Current Compensation Using Multiple Distributed Resources

3.1 Harmonic current compensation

The concept of harmonic current compensation using multiple DRs is illustrated in Fig. 7. The central controller has three major function blocks: the harmonic current identifier, the power margin calculator and the participation factor calculator. When the harmonic problem is detected by a local monitor, the request for the harmonic compensation is transferred to the harmonic current identifier of the central controller with the information of the distorted current waveform. Then, the harmonic identifier calculates the harmonic components and the harmonic apparent power to be compensated.

The power margin calculator obtains the instantaneous power margin of DRs, which means the compensation capability of the DRs. The details of the power margins will be explained in Section 3.3.

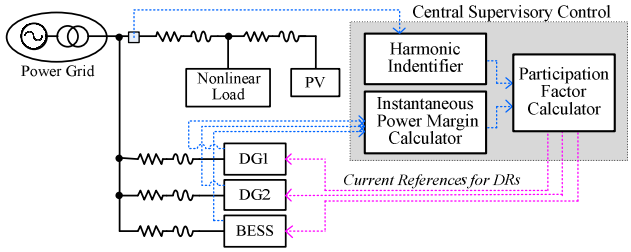

Fig. 7. Configuration of the proposed harmonic current compensation strategy

Then, the output of the two function blocks such as the total amount for harmonic current to be compensated and the maximum harmonic compensation level of each DR are delivered to the participation factor calculator. This participation factor calculator determines the participation factor of harmonic current compensation of each DR in consideration of multiple objectives. In this paper, fuzzy-based multi-objective optimization model is applied to the participation factor calculator. The details of the optimization algorithm will be presented in Section 3.4

3.2 Harmonic current identification

This paper borrows the harmonic current identification method from the previous researches such as [22-23]. The harmonic identification method uses adaptive detection method to analyze the input signal into individual harmonic components. This method can be mathematically derived by strictly positive real Lyapunov method.

The nonlinear load current (i_L) can be decomposed into its harmonic components as

$$\begin{aligned} i_L &= I_{dc} + I_1 \sin(\omega_1 t + \varphi_1) + \sum_{k=2}^{n} I_k \sin(\omega_k t + \varphi_k) \\ &= I_{dc} + \sum_{k=1}^{n} \left(I_{k1} \sin \omega_k t + I_{k2} \cos \omega_k t \right) \end{aligned} \quad (1)$$

where I_{dc} is the dc component; I_k, ω_k, and φ_k represent the magnitude, angular frequency, and phase angle of the k_{th} harmonic component, respectively; by the sine and cosine formula, $I_{k1} = I_k \cos\varphi_k$ and $I_{k2} = I_k \sin\varphi_k$.

If the bandwidth of the current measurement is sufficiently large, Eq. (1) can be expressed in the parametric model as

$$i_L = \theta^T \phi \quad (2)$$

where $\theta = [I_{11}, I_{12}, \cdots, I_{n1}, I_{n2}, I_{dc}]^T$

$$\phi = [\sin \omega_1 t, \cos \omega_1 t, \cdots, \sin \omega_n t, \cos \omega_n t, 1]^T$$

The objective function $J(\theta)$ of the harmonic current identifier uses the square of the estimation error as

$$J(\theta) = \frac{\varepsilon^T \varepsilon}{2} = \frac{\left(i_L - \hat{\theta}^T \phi\right)^T \left(i_L - \hat{\theta}^T \phi\right)}{2} \quad (3)$$

where the notation ($\wedge$) means the estimate of the parameter; the estimation error is defined as $\varepsilon = i_L - \hat{i}_L = (\theta - \hat{\theta})^T \phi$. By applying the gradient method to minimize the objective function, the adaptive formulas for estimation of each individual component in $\hat{\theta}$ are obtained as

$$\dot{\hat{I}}_{k1} = \gamma_{k1} \varepsilon \sin \omega_k t, \quad \dot{\hat{I}}_{k2} = \gamma_{k2} \varepsilon \cos \omega_k t, \quad \dot{\hat{I}}_{dc} = \gamma_{dc} \varepsilon \quad (4)$$

where γ_{k1}, γ_{k2}, and γ_{dc} are the adaptive gains, which are positive numbers. The convergence of the update laws in (4) is rigorously guaranteed by evaluation of the persistent excitation condition [23]. The estimates of the amplitude $\hat{I}_n(t)$ and the phase angle $\hat{\varphi}_n$ of the harmonic components can be calculated by

$$\hat{I}_n(t) = \sqrt{\hat{I}_{n1}^2(t) + \hat{I}_{n2}^2(t)}, \quad \hat{\varphi}_n(t) = \cos^{-1}\left(\frac{\hat{I}_{n1}(t)}{\hat{I}_n(t)}\right) \quad (1)$$

The fundamental frequency, ω_1, varies according to the system power balance. It should be updated and then applied to each harmonic estimation process. The update law of the fundamental frequency (ω_1) can also be developed by gradient method with a least square error objective function. The objective function is calculated as

$$\begin{aligned} J(\omega_1) &= \frac{1}{2}\left[i_L - \hat{i}_L \right]^2 \\ &= \frac{1}{2}\left[i_L - \left\{ \sum_{k=1}^{n} \left(\hat{I}_{k1} \sin k\omega_1 t + \hat{I}_{k2} \cos k\omega_1 t \right) + \hat{I}_{dc} \right\} \right]^2 \end{aligned} \quad (6)$$

Then, the update law of the fundamental frequency can be obtained as

$$\dot{\omega}_1 = -\alpha \varepsilon \left[\sum_{k=1}^{n} kt \cdot \left(\hat{I}_{k1} \cos k\omega_1 t - \hat{I}_{k2} \sin k\omega_1 t \right) \right] \quad (7)$$

where α is an adaptive gain.

3.3 Instantaneous power margin

The apparent power of the load ($|S_L|$) can be obtained as

$$|S_L| = 3 V_L^{rms} I_L^{rms} \quad (8)$$

where V_L^{rms} and I_L^{rms} are the root-mean-square (rms) values of the phase voltage and the line current of the load, respectively. Normally, the rms voltages of power grids should be regulated tightly within ± 3~5%.

If we assume that the harmonic components in the

voltage can be neglected, the apparent power of the nonlinear load is dominated by the rms current. The rms current can be expressed as

$$\begin{aligned} I_L^{rms} &= \sqrt{\frac{1}{T}\int_0^T i_L^2(t)} \\ &= \sqrt{\frac{1}{T}\int_0^T \left[\sum_{k=1}^{\infty} I_k \sin\left(\omega_k t+\varphi_k\right)\right]\left[\sum_{k=1}^{\infty} I_k \sin\left(\omega_k t+\varphi_k\right)\right] dt} \\ &= \sqrt{\left(\frac{I_1}{\sqrt{2}}\right)^2 + \sum_{k=2}^{\infty}\left(\frac{I_k}{\sqrt{2}}\right)^2} = \sqrt{\left(I_1^{rms}\right)^2 + \sum_{k=2}^{\infty}\left(I_k^{rms}\right)^2} \\ &= \sqrt{\left(I_1^{rms}\right)^2 + \left(I_h^{rms}\right)^2} \end{aligned} \tag{9}$$

where I_1, I_k, ω_k, and φ_k are the same as (1); I_1^{rms} and I_h^{rms} are the rms values of the fundamental component and the harmonic components of the load current [8].

If we apply (9) to (8), then the harmonic apparent power of the load $\left|S_h^m\right|$ can be obtained as

$$\left|S_h^m\right| = \sqrt{\left|S_L\right|^2 - \left|S_1\right|^2} \tag{10}$$

where $\left|S_1\right| = 3V_L^{rms} I_1^{rms}$ and $\left|S_h\right| = 3V_L^{rms} I_h^{rms}$.

When DRs compensate harmonic components, they should inject additional current to the microgrid during harmonic compensation. This means that the capability of harmonic compensation of a DR depends on the instantaneous power margin, which is defined as the difference between the rated apparent power of the DR and the injecting apparent power. The instantaneous power margin of DR unit *i* can be calculated as

$$\left|S_{DR_i}^{\text{margin}}\right| = \left|S_{DR_i}^{rated}\right| - 3 \cdot V_{DR_i}^{rms} \cdot I_{DR_i}^{rms} \tag{11}$$

where, V_i^{rms} and I_i^{rms} are the rms values of the phase voltage and the line current of the DR_i, respectively; $\left|S_{DR_i}^{rated}\right|$ is the rated apparent power of DR_i.

3.4 Coordination method of multiple DRs

3.4.1 Objectives of Coordination

As previously seen, when DRs compensate harmonics, apparent power is to be injected to the grid. On the other hand, the power injection capability of the power inverters is limited. Therefore, when a DR supplies electric power close to its rating, its harmonic compensation function should be limited. Hence, the instantaneous power margin of DRs is the most important factors to determine the harmonic compensation level of each DR. In addition, the generation cost and types of DRs are another important issue because the operation strategies might be quite different based on them. To solve these multiple objectives more intelligently, an intelligent coordination method that can efficiently handle multiple objectives is required for harmonic compensation using multiple and various DRs.

This paper proposes fuzzy-based multi-objective nonlinear optimization algorithm to coordinate multiple DRs for harmonic compensation. The objectives for the fuzzy optimization are as follows:

The harmonic distortion in the source current at the point of common coupling (PCC) should be minimized by the harmonic compensation.

When the SOC of the BESS is large enough, the BESS has priority to DGs in harmonic compensation.

The SOC of the BESS should be kept within 30~100% [18]. As the SOC of the BESS decreases below 80%, the satisfaction of compensation of BESS decreases with a variable slope.

The harmonic compensation capability of a DR depends on its remaining power margin. If the remaining power margin of a DR is exhausted, the degree of the harmonic compensation of the DR should be reduced faster than other DRs that hold more power margins.

Whereas the previous research as in [8] considered only the power margins, the optimization method proposed in this paper can consider multiple objectives within integrated fuzzy optimization algorithm.

3.4.2 Fuzzy Optimization Problem

The proposed multi-objective optimization algorithm determines the degree of harmonic compensation of each DR to minimize the harmonics at the PCC and maximize the satisfaction degree of the multiple objectives using fuzzy system. In a fuzzy system, the degrees of satisfaction of the corresponding objectives are represented by fuzzy membership functions [24-27]. Let us define the fuzzy set F_i to represent the i_{th} objective function as

$$F_i = \int_x \mu_{F_i}(x_i) \Big| x_i \tag{12}$$

where x_i is the harmonic compensation power of unit *i* and $\mu_{F_i}(x_i)$ is the fuzzy membership function of x_i in F_i. $\mu_{F_i}(x_i)$, which is also called the degree of satisfaction for F_i, characterizes either objective or constraint function. The definition of the fuzzy membership functions will be explained as follows.

3.4.3 Membership Function of DR Satisfaction

Let us define the fuzzy set X_i as the harmonic compensation degree of DR unit *i*. The fuzzy set X_i is defined in $[0, x_i^m]$ where x_i^m is the maximum apparent power that can be used for harmonic compensation of unit *i*, x_i^m is the same as the instantaneous power margin of unit *i*. Then, let us define the membership function, $\mu_{X_i}(x_i)$ using the S-function, which means the satisfaction degree

of the DR, as follows.

If $a_i \geq 0$,

$$\mu_{X_i}(x_i) = \begin{cases} 1 & 0 \leq x_i \leq a_i \\ 1 - 2\left(\frac{x_i - a_i}{x_i^m - a_i}\right)^2 & a_i \leq x_i \leq \frac{a_i + x_i^m}{2} \\ 2\left(\frac{x_i - x_i^m}{x_i^m - a_i}\right)^2 & \frac{a_i + x_i^m}{2} \leq x_i \leq x_i^m \end{cases} \quad (13)$$

Otherwise,

$$\mu_{X_i}(x_i) = \begin{cases} 1 - 2\left(\frac{x_i - a_i}{x_i^m - a_i}\right)^2 & 0 \leq x_i \leq \frac{a_i + x_i^m}{2} \\ 2\left(\frac{x_i - x_i^m}{x_i^m - a_i}\right)^2 & \frac{a_i + x_i^m}{2} \leq x_i \leq x_i^m \end{cases} \quad (14)$$

where the parameter a_i is decided as $a_i = x_i^m - c_i$ where c_i is the parameter for the S-function that can be determined heuristically. The value c_i used in this paper will be provided in Section 4.

The membership function means if the DR uses less harmonic compensation power, the satisfaction degree increases. When the DR has enough power margins, the membership function is of the form as Fig. 8(a). In this case, when the DR injects the apparent power less than a_i, the satisfaction degree is equal to 1, which is maximum satisfaction degree. When the instantaneous power margin of the DR is reduced, the membership function is shifted to the left as shown in Fig. 8(b). In this case, the maximum satisfaction is less than 1.

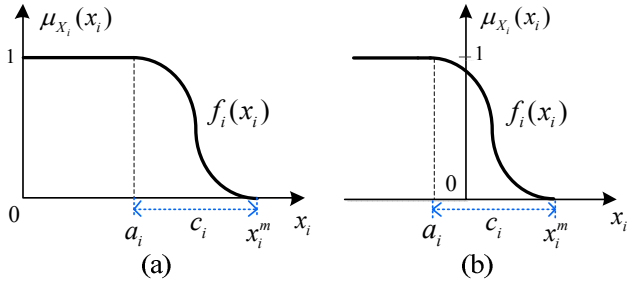

Fig. 8. Membership function of DR unit i:
(a) $a_i \geq 0$, (b) $a_i < 0$

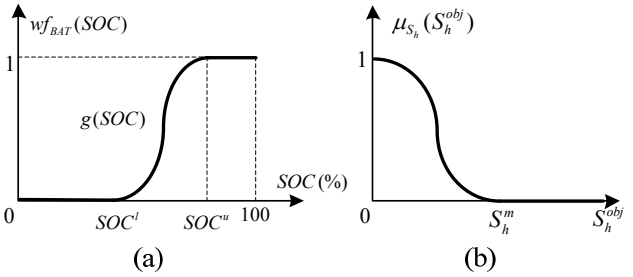

Fig. 9. Weighting and membership functions: (a) The weighting function of BESS, (b) the membership function of uncompensated harmonic power

3.4.4 Weighting Function Considering SOC of BESS

The SOC of the BESS can be considered as a weighting function to the membership function of the BESS. The weighting function of the SOC is defined as

$$wf_{BAT}(SOC) = \begin{cases} 0 & 0 \leq SOC \leq SOC^l \\ g(SOC) & SOC^l \leq SOC \leq SOC^u \\ 1 & SOC^u \leq SOC \leq 100 \end{cases} \quad (15)$$

where SOC^l and SOC^u are lower/upper bound that are defined in [0,100], respectively and the function g is a S-function as shown in Fig. 9(a). In this paper, the lower and upper bounds are set to 40% and 80%, respectively.

The weighting function is multiplied to the membership function of the BESS expressed as (13) and (14). Therefore, if the SOC of a BESS is decreased, the satisfaction degree of the BESS is also reduced.

3.4.5 Membership Function of Uncompensated Harmonics

The degree of system-wide satisfaction of the harmonic compensation can be measured by the uncompensated harmonic power ($|S_h^{obj}|$) at the PCC that can be defined as

$$|S_h^{obj}| = |S_h^m| - \sum_i x_i \quad (16)$$

where $|S_h^m|$ is defined as (16). This means that the smaller the uncompensated harmonic power $|S_h^{obj}|$ is, the better the harmonic compensation performance is.

The membership function of harmonics is defined in $[0, S_h^m]$ and it can be expressed in a decreasing function as shown in Fig. 9(b) and defined as

$$\mu_{S_h}(S_h^{obj}) = \begin{cases} 1 - 2\left(\frac{S_h^{obj}}{S_h^m}\right)^2 & 0 \leq S_h^{obj} \leq \frac{S_h^m}{2} \\ 2\left(\frac{S_h^{obj} - S_h^m}{S_h^m}\right)^2 & \frac{S_h^m}{2} \leq S_h^{obj} \leq S_h^m \end{cases} \quad (17)$$

3.4.6 Multi-objective optimization using Fuzzy Sets

The multi-objective optimization model in fuzzy environment is constructed to determine the harmonic compensation power (x_i) of unit *i*. According to the max-min principle, the decision function *D*, that is the degree of overall satisfaction, is the minimum of all membership values [25-27]. In addition, the optimal solution $\mathbf{x}^*$ can be obtained when $\mu_D(\mathbf{x}^*)$ is maximized where $\mathbf{x}$ is a vector of x_i.

$$\mu_D(\mathbf{x}^*) = \max_{\mathbf{x}} \min[\mu_{X_1}(\mathbf{x}), \mu_{X_2}(\mathbf{x}), \mu_{X_3}(\mathbf{x}), \mu_{S_h}(\mathbf{x})] \quad (18)$$

Then, the participation factors in the harmonic compensation of the DRs can be obtained as

$$pf(\mathbf{x}^*) = \frac{\mathbf{x}^*}{S_h^m} \tag{19}$$

4. Simulation Studies

The microgrid system including a PV system, two inverter-based DGs, a BESS, and a nonlinear load was developed using MATLAB/Simulink. The single-line diagram of the microgrid is shown in Fig. 10. The power system data such as transformers and cables were determined with reference to the microgrid pilot plant of Korea Electric Power Company [28]. The nonlinear loads whose overall rating is around 100kVA consist of a DC load using a diode-rectifier and a thyristor-converter for motor driving circuit, which are notorious for significant harmonic current absorption. The 10kVA PV system is connected adjacent to the load and controlled by the MPPT algorithm with unity power factor. DG1 and DG2 are inverter-interfaced DGs that contain the controller explained in Fig. 6. The power inverters for DG1 and DG2 meet the IEEE standard 1547 for interconnecting DGs with the power grids. Micro-gas-turbines (MGTs) are used as energy resources for DG1 and DG2. The detailed information of the MGTs is provided in [28].

DG1, DG2, and BESS can participate in the harmonic compensation in this study. The power rating of DG1, DG2, and BESS are set to 30kVA, 30kVA, and 40kVA, respectively. For simplicity in calculation, all the variables in the microgrid are expressed in per unit values with the 100kVA power base and 380V line-to-line voltage base.

The parameters of the fuzzy membership functions are set up as follows: the maximum satisfaction degrees of all the membership functions are set to 1. The parameter c_i in (13) and (14) are set to 0.15, 0.15, and 0.05 for DG1, DG2, and BESS, respectively. Because the full output power of DG1 can be expressed as 0.3 p.u. (30kVA with 100kVA base), the c_i value 0.15 of DG1 means the satisfaction degree of harmonic compensation of DG1 decreases when the instantaneous power margin of DG1 is less than 50% of its rated value. Similarly, the c_i value 0.05 of BESS means that the satisfaction degree reduces when the instantaneous power margin of BESS is less than 12.5% of the rated power. The lower/upper bounds that are weighting function parameters of BESS are chosen as 40% and 80%, respectively.

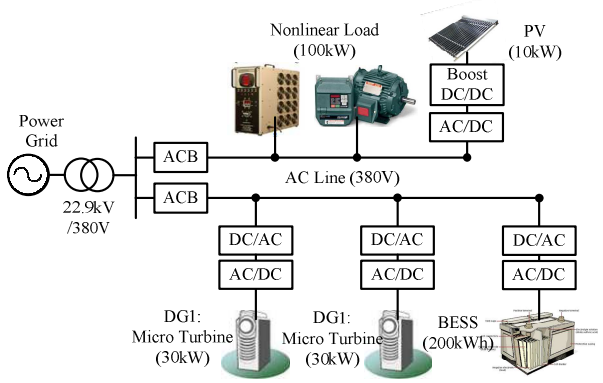

Fig. 10. Microgrid system model for simulation study

To demonstrate the effectiveness of the proposed method, four cases are examined with different conditions via simulation studies. These representative conditions of the cases are described in Table 1. The parameters P_{DG1}, P_{DG2}, and P_{BESS} means the fundamental power output of DG1, DG2, and BESS with unity power factor in per unit based on their own rated power bases, respectively. For example, the parameter $P_{DG1}(=0.5)$ in Case I means that the normal output power of DG1 is 15kVA ($=0.5\times 30\text{kVA}$).

Table 1. DR operating conditions of three case studies

Parameters	Case I	Case II	Case III	Case IV
$P_{DG1}[p.u.]$	0.5	0.7	0.9	0.5
$P_{DG2}[p.u.]$	0.5	0.6	0.8	0.5
$P_{BESS}[p.u.]$	0.5	0.5	0.8	0.7
$SOC_{BESS}[\%]$	79%	75%	50%	75%

※ The power base of the per unitization is based on their own rating (DG1:30kVA, DG2:30kVA, BESS:40kVA)

In Case I, all the DRs have enough power margins and the battery SOC is also enough. In Case II, the normal output power of DG1 is larger than DG2 while the BESS still have enough power margin as well as the stored energy. In Case III, most DRs generate output power close to their ratings and the SOC of the battery approaches the lower boundary 40%. In all cases, the size of the nonlinear load is set to 100kVA. In Case IV, all the DRs and the battery have enough power margins as in Case I. The purpose of the simulation study of Case IV is conducted to investigate the performance of the proposed method in different loading conditions.

The optimization results of the four cases using the proposed fuzzy-based multi-objective optimization are listed in Table 2. Since the DRs have different power ratings, the values in Table 2 are standardized with 100kVA power base. For example, in Case I, the x_1 value 0.0168 p.u. means that DG1 supplies 1.68 kW harmonic compensation that is also 0.056 p.u. considering its own power rating 30kVA. As stated above, in Case I, all the DRs have enough power margins for harmonic compensation. Therefore, the uncompensated harmonic power (S_h^{obj}) is zero after compensation. It can also be seen that the BESS compensates more harmonics than the other DGs. The participation factors of DG1, DG2, and BESS are 25%, 25%, and 50%, respectively. This result is consistent with the fundamental ideas of the coordination as explained in section 3.4.1. This means that the fuzzy

Table 2. Simulation results with fuzzy-based multi-objective optimization for three case studies

Variables	Case I	Case II	Case III	Case IV
Injected harmonic power of DG1 (x_1) [p.u.]	0.0168	0.0	0.0	0.0375
Injected harmonic power of DG2 (x_2) [p.u.]	0.0168	0.0075	0.0070	0.0375
Injected harmonic power of BESS (x_3) [p.u.]	0.0336	0.0597	0.030	0.0233
Uncompensated harmonic power at PCC (S_h^{obj}) [p.u.]	0.0	0.0	0.0302	0.0
Satisfaction degree of DG1 ($\mu_{X_1}(x_1)$)	0.975	1.0	1.0	0.875
Satisfaction degree of DG2 ($\mu_{X_2}(x_2)$)	0.975	0.875	0.250	0.875
Satisfaction degree of BESS ($wf \cdot \mu_{X_3}(x_3)$)	0.975	0.875	0.250	0.875
Satisfaction degree of uncompensated harmonic power ($\mu_{S_h}(S_h^{obj})$)	1.0	1.0	0.5961	1.0
Participation factor of DG1 ($pf(x_1)$) [%]	25.0	0	0	38.15
Participation factor of DG2 ($pf(x_2)$) [%]	25.0	11.16	10.42	38.15
Participation factor of BESS ($pf(x_3)$) [%]	50.0	88.84	44.64	23.70
Total sum of participation factors ($\sum pf(x_k)$) [%]	100.0	100.0	55.06	100.0

※ The power base of the per unitization is 100kVA.

membership function and the optimization process are well-defined.

Fig. 11 shows the simulation results of Case I using the proposed coordination method. The harmonic compensation of DRs starts at 1.0 sec. Before the harmonic compensation, the source current shown in Fig. 11(a) contains significant harmonics. However, after 1.0 sec, the source current becomes sinusoidal. DRs compensate harmonic currents according to their participation factors. Since the participation factors and the normal power output of DG1 and DG2 are equal, their output currents have the same waveform as shown in Figs. 11 (c) and (d). It can be noted that BESS compensates more harmonics than DGs.

In Case II, The power margin of DG1 is the smallest among the DRs. The power margin of BESS and the battery SOC are large enough. Therefore, the participation factors are assigned as 0%, 11.16%, and 88.84% to DG1, DG2, and BESS, respectively. Since the total sum of the participation factors is 100%, the uncompensated harmonic power at the PCC can be eliminated to zero. This harmonic compensation results can be confirmed by the simulation results shown in Fig. 12. The source current can be fully compensated after the harmonic compensation as shown in Fig. 12(a). Since DG1 does not participate in the harmonic

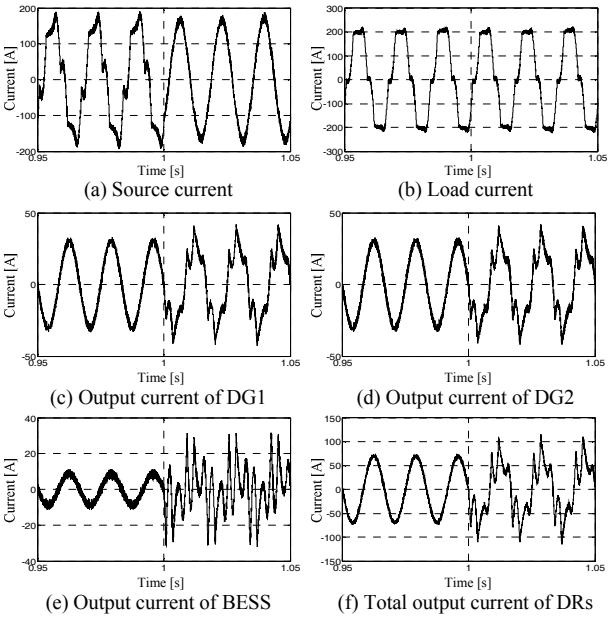

Fig. 11. Simulation results - Case I

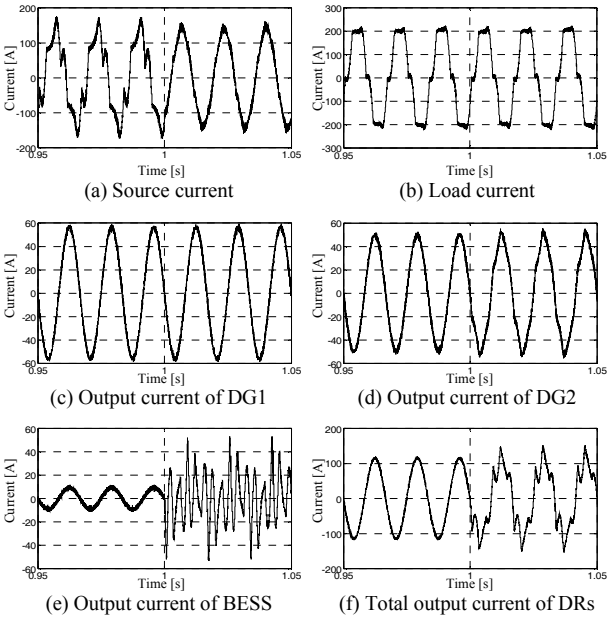

Fig. 12. Simulation results – Case II

compensation, the output current is sinusoidal as shown in Fig. 12(c). BESS compensates most harmonic components as Fig. 12(e).

In Case III, most DRs have not enough power margins and the battery SOC is 50% that is close to its lower boundary 40%. In this case, the total sum of the participation factors of DRs is 55.06%, which is less than 100%. Therefore, the harmonic current cannot be completely compensated. Fig. 13 shows the simulation results of Case III. As shown in Fig. 13(a), the harmonic components in the source current cannot completely be

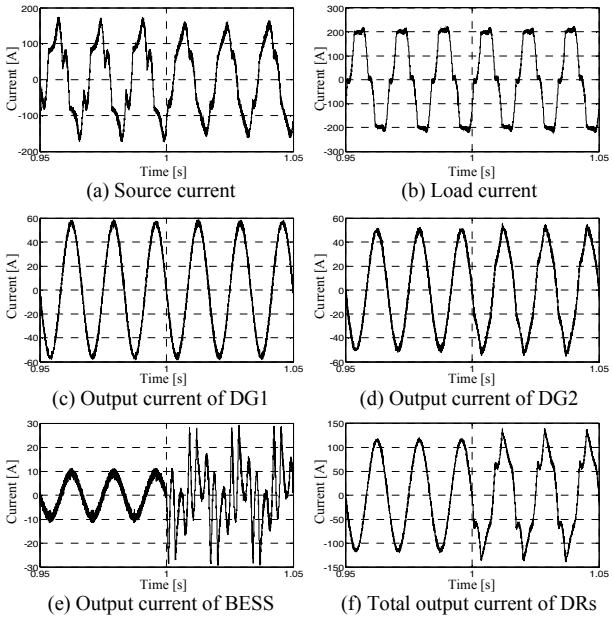

Fig. 13. Simulation results – Case III

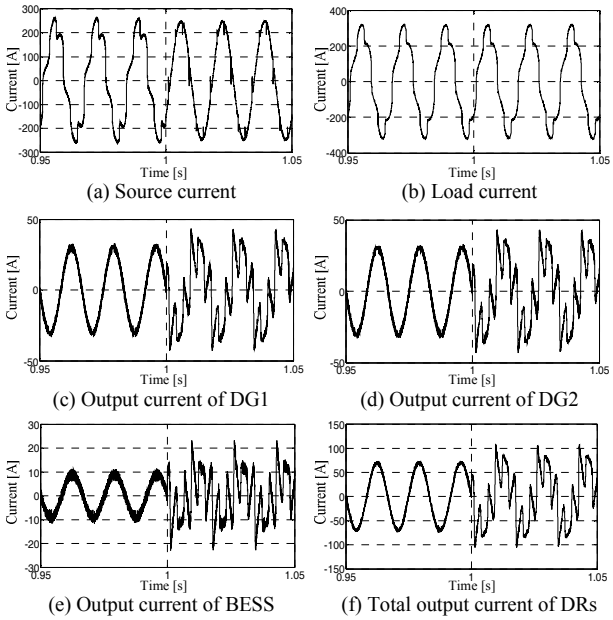

Fig. 14. Simulation results – Case IV

eliminated after harmonic compensation because the DRs operate in close proximity to their rated power.

In Case IV, we applied different nonlinear loads to investigate the performance of the proposed method. While a diode-rectifier, which is one of the most popular interface technologies, draws harmonic currents from Case I to Case III, we added a thyristor-based motor-drive load to the diode-rectifier [29]. Fig. 14(b) shows the load current that contains different harmonic components from the previous cases. The power outputs of DG1 and DG2 are the same as those of Case I but the power output of the BESS is 70%, which is different from Case I. Therefore, the participation factors of DG1 and DG2 slightly increase compared to Case I. Because the total sum of the participation factors of DGs and the BESS is 100%, most harmonic components in the source current can be eliminated as shown in Fig. 14(a).

The total power margin of DRs of Case III is larger than the harmonic apparent power of the load. Therefore, ideally, the harmonic components can be fully compensated. However, Table 2 shows that the harmonics are partially compensated. This is because the satisfaction degree of the membership functions is designed to preserve the power margins of DRs and the battery SOC conservatively. In other words, if we change the parameters c_i to smaller values, the DRs will compensate harmonics more aggressively using more power margins. Therefore, the membership function design should be done corresponding to the DR operation strategies.

5. Conclusion

A new intelligent coordination method for harmonic compensation using multiple DRs was proposed and discussed in this paper. The proposed method suggests that the harmonic compensation using the remaining power margins of DRs and the energy stored in the BESSs. The coordination of multiple DRs is not simple because their operating conditions and objectives are various. This paper proposed a fuzzy-based multi-objective optimization model for the intelligent DR coordination. The details in the membership function design were provided and the performance of the proposed method was verified via simulation studies using developed dynamic switching model of the microgrid.

Acknowledgements

This work was supported by the Ministry of Knowledge Economy, Korea, under the Information Technology Research Center support program (NIPA-2012-H0301-12-2007) supervised by the National IT Industry Promotion Agency, the power generation and electricity delivery of the Korea Institute of Energy Technology Evaluation and Planning (KETEP) grant funded by the Korea government Ministry of Knowledge Economy (20111020400080) and Basic Science Research Program through the National Research Foundation of Korea funded by the Ministry of Education, Science and Technology (2012-0003555).

References

[1] J. Arrillaga and N.R. Watson, Power System Harmonics: John Wiley and Sons, 2003.

[2] E.F. Fuchs and M.A.Masoum, Power Quality in

Power Systems and Electrical Machines, Academic Press, 2008.
[3] Power System Harmonics, Rockwell Automation, 2001.
[4] Recommended Practices and Requirements for Harmonic Control in Electric Power Systems, IEEE Standard 519, 1992
[5] Assessment of Emission Limits for Distorting Loads in MV and HV Power Systems, IEC 1000-3-6, 1996.
[6] H. Fujuta and H. Akagi, "The Unified Power Quality Conditioner: The Integration of Series- and Shunt-Active Filters," IEEE Trans. Power Electronics, Vol. 13, No. 2, pp. 315-322, Mar. 1998.
[7] S. Bhattacharya, T.M. Frank, D.M. Divan, B. Banerjee, "Active filter system implementation," IEEE Industry Application Magazine, Vol. 4, No. 5, pp. 47-63, Sep/Oct. 1998.
[8] S. Leng, I. Chung, C.S. Edrington, and D.A. Cartes, "Coordination of Multiple Adjustable Speed Drives for Power Quality Improvement," Electric Power Systems Research, Vol. 81, No. 6, pp. 1227-1237, Jun. 2011.
[9] R.H. Lasseter, "Control and Design of Microgrid Components," PSERC Final Report, Jan. 2007.
[10] N. Hatziargyriou, H. Asano, R. Iravani, and C. Marnay, "Microgrids," IEEE Power & Energy Magazine, pp. 78-94, Jul./Aug. 2007.
[11] I. Chung, W. Liu, D. Cartes, E. Collins, and S. Moon, "Control Methods for Multiple Distributed Generators in a Microgrid System," IEEE Trans. Industry Applications, Vol. 46, No. 3, pp. 1078-1088, May/June 2010.
[12] J.A. Lopes, N. Hatziargyriou, J. Mutale, P. Djapic, and N. Jenkins, "Integrating distributed generation into electric power systems," Electric Power Systems Research, Vol. 77, No. 9, pp. 1189-1203, Jul. 2007.
[13] K. Nguyen, D. Won, S. Ahn, and I. Chung, "Power Sharing Method for a Grid-Connected Microgrid with Multiple Distributed Generators," Journal of Electrical Engineering & Technology, Vol. 7, No. 4, pp. 459-467, July 2012.
[14] R. Liang and Y. Wang, "Fuzzy-Based Reactive Power and Voltage Control in a Distribution System," IEEE Trans. Power Delivery, Vol. 18, No. 2, pp. 610-618, Apr. 2003.
[15] B. Venkatesh, G. Sadasivam, and M. Khan, "A new optimal reactive power scheduling method for loss minimization and voltage stability margin maximization using successive multi-objective fuzzy LP technique," IEEE Trans. Power Systems, Vol. 15, No. 2, pp. 844-851, May. 2000.
[16] Y. Huang, "Enhanced genetic algorithm-based fuzzy multi-objective approach to distribution network reconfiguration," Generation, Transmission and Distribution, IEE Proceedings, Vol. 149, No. 5, pp. 615-620, Sep. 2002.
[17] Y. Ji, J. Kim, S. Park, J. Kim, and C. Won, "C-language based PV array simulation technique considering effects of partial shading," IEEE International Conference on Industrial Technology 2009, pp. 1-6, Feb. 2009.
[18] X. Liu, L. Lopes, "An improved perturbation and observation maximum power point tracking algorithm for PV arrays," Proc. of the IEEE 35th Anuual Power Electronics Specialists Conference 2004, Vol. 3, pp. 2005-2010.
[19] H. Lee, W. Chae, J. Park, J. Kim, and C. Kim, "The development & performance test of 10kW power conditioning system for microgrid," Journal of the Korean Institute of Illuminating and Electrical Installation Engineers, Vol. 26, No. 7, pp. 55-62, 2011.
[20] J. Kwon, K. Nam, and B. Kwon "Photovoltaic Power Conditioning System With Line Connection," IEEE Trans. Industrial Electronics, Vol. 53, No. 4, pp. 1048-1054, 2006.
[21] S. Teleke, M. Baran, S. Bhattacharya, and A. Huang, "Rule-Based Control of Battery Energy Storage for Dispatching Intermittent Renewable Sources," IEEE Trans. Sustainable Energy, Vol. 1, No. 3, pp. 117-124, Oct. 2010.
[22] L. Qian, D. Cartes, H. Li, "An improved adaptive detection method for power quality improvement," IEEE Trans. Ind. Appl. 44 (2) (2008) 525-533.
[23] S. Leng, W. Liu, I. Chung, and D. Cartes, "Active power filter for three-phase current harmonic cancellation and reactive power compensation," in Proc. American Control Conference, St. Louis, Missouri, June 10-12, 2009, pp. 2140-2147
[24] H.Z. Huang, "Fuzzy multi-objective optimization decision-making of reliability of series system," Microelectron. Reliab., Vol. 37, No. 3, pp. 447-449, 1997.
[25] R.A. Ribeiro, "Fuzzy multiple attribute decision making: A review and new preference elicitation techniques," Fuzzy Sets and Systems, Vol. 78, pp. 155-181, 1996.
[26] T.J. Ross, Fuzzy logic with engineering applications, 3rd ed. Wiley, 2010.
[27] R.E. Bellman and L.A. Zadeh, "Decision-making in a fuzzy environment,' Management Science, Vol. 17, No. 4, pp. 141-164, 1970.
[28] C. Yoo, I. Chung, S. Hong, W. Chae, and J. Kim, "A Feasibility Study on DC Microgrids Considering Energy Efficiency," The Transactions of the KIEE, Vol. 60, No. 9, pp. 1674-1683, Sep. 2011.
[29] R. Chan, J. Crider, C. Harianto, J. Lian, J. Neely, S. Pekarek, S. Sudhoff, and N. Vaks, "A Medium Voltage DC Testbed for Ship Power System Research," ESTS 2009, pp. 560-567.

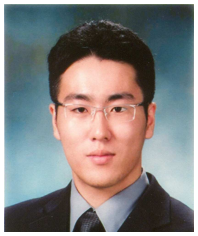

Hyun-Koo Kang received his B.S. and M.S. degrees in electrical engineering from Seoul National University, Seoul, Korea, in 2005 and 2007, respectively, where he is currently pursuing the Ph.D. degree. His research interests are power quality, distributed energy resources, and operation of microgrid.

Cheol-Hee Yoo received the B.S. and M.S. degrees in electronics engineering from Kookmin University, Seoul, Korea, in 2007 and 2009, respectively, where he is currently working toward his Ph.D. degree. His research interests are in the areas of microgrids, renewable energy applications, hardware-in-the-loop simulation, multi-agent system, and high-efficiency power converters.

Il-Yop Chung received his B.S., M.S., and Ph.D. degrees in electrical engineering from Seoul National University, Seoul, Korea, in 1999, 2001, and 2005, respectively. He was a Postdoctoral Associate at Virginia Tech, Blacksburg, VA, from 2005 to 2007. From 2007 to 2010, he worked for the Center for Advanced Power Systems at Florida State University, Tallahassee, FL as an Assistant Scholar Scientist. Currently, he is an Assistant Professor at Kookmin University, Seoul, Korea. His research interests are power quality, distributed energy resources, renewable energy, and shipboard power systems.

Dong-Jun Won received B.S., M.S., and Ph.D. degrees in Electrical Engineering, Seoul National University, Seoul, Korea in 1998, 2000, and 2004 respectively. He was a Postdoctoral Fellow with the APT Center, University of Washington, Seattle, WA, USA. Currently, he is an Associate Professor with the School of Electrical Engineering, INHA University, Incheon, Korea. His research interests include power quality, microgrid, renewable energy, and smart grid.

Seung-Il Moon received the B.S. degree in electrical engineering from Seoul National University, Seoul, Korea, in 1985, and the M.S. and Ph.D. degrees in Electrical Engineering from Ohio State University, Columbus, OH, USA in 1989 and 1993, respectively. Currently, he is a Professor of the School of Electrical Engineering and Computer Science at Seoul National University. He is the Editor-in-Chief of Journal of Electrical Engineering and Technology and also the Vice Chairman of Editorial Board of the Korean Institute of Electrical Engineers (KIEE) since 2008. His special fields of interest include power quality, flexible ac transmission system, renewable energy, and distributed generation.